Hybrid Materials Hot Paper

International Edition: DOI: 10.1002/anie.201501941
German Edition: DOI: 10.1002/ange.201501941

Polyoxometalate Complexes of Anatase-Titanium Dioxide Cores in Water**

*Manoj Raula, Gal Gan Or, Marina Saganovich, Offer Zeiri, Yifeng Wang, Michele R. Chierotti, Roberto Gobetto, and Ira A. Weinstock**

Abstract: *Polyoxometalate (POM) cluster anions are shown to serve as covalently coordinated ligands for anatase-TiO_2 nanocrystals, giving isolable assemblies uniquely positioned between molecular macroanions and traditional colloidal nanoparticles. Na^+ salts of the water-soluble polyanionic structures are obtained by reacting amorphous TiO_2 with the 1 nm lacunary ion, $Na_7[\alpha\text{-}XW_{11}O_{39}]$ ($X = P^{5+}$), at 170 °C, after which an average of 55 $\alpha\text{-}PW_{11}O_{39}^{7-}$ clusters are found as pentadentate ligands for Ti^{IV} ions covalently linked to 6 nm single-crystal anatase cores. The attached POMs are reversible electron acceptors, the reduction potentials of which shift in a predictable fashion by changing the central heteroatom, X, directly influencing a model catalytic reaction. Just as POM cluster anions control the reactivities of metal centers in molecular complexes, directly coordinated POM ligands with tunable redox potentials now provide new options for rationally controlling the reactions of semiconductor nanocrystals.*

Polyoxometalates[1] (POMs) serve as oxygen-donor ligands for mono-, di-, tri-, and small-nuclearity oxide- and hydroxide-linked fragments of reactive transition (d-block) and main-group (p-block) metal ions, providing molecular complexes that catalyze a variety of oxidative and other processes. In many cases, catalytic activity emerges from the unique properties of the cluster anions, often derivatives of plenary Keggin or Well–Dawson structures, that serve as ligands for the reactive metal centers. This is true as well for POM complexes of Ti^{IV} ions,[2] some of which catalyze photochemical reductions of CO_2 to methane,[3] and selective oxidations by H_2O_2.[4]

Structurally, a general feature of oxophilic Ti^{IV} centers in molecular complexes is their natural tendency to form high-nuclearity oxide-bridged cores. Reported examples include POM complexes, such as $[(\alpha\text{-}Ti_3SiW_9O_{37}OH)_3(TiO_3(OH_2)_3)]^{17-}$[2d] and $[(\alpha\text{-}1,2,3\text{-}P_2W_{15}Ti_3O_{62})_4\{\mu_3\text{-}Ti(OH)_3\}_4Cl]^{45-}$,[5] with cores of 10 and 16 Ti^{IV} atoms, respectively, while up to 34 Ti atoms[6] are found in molecular titanium oxide clusters capped by alkoxide and other[7] organic anions. Notably, ligand-capped titanium oxide clusters are fundamentally important molecular models for TiO_2 semiconductors.[6,7]

We now report a conceptually new role for POM cluster anions as covalently coordinated redox-active ligands in polyanionic complexes of TiO_2-semiconductor nanocrystals themselves (Scheme 1). Multiple lines of evidence from solid- and solution-state analytical methods unequivocally demonstrate that numerous Ti^{IV}-substituted mono-defect Keggin-ion capping ligands, $[\alpha\text{-}PW_{11}O_{39}Ti]\text{–}O^-$, are covalently attached to ca. 6 nm anatase-TiO_2 cores (each comprised of 1800 ± 550 Ti atoms), resulting in isolable, water-soluble nanostructures uniquely positioned between molecular macroanions[2a,5] and more traditional, electrostatically stabilized, colloidal metal oxides.[8] Moreover, the covalently attached POMs serve as tunable electron acceptors at the surfaces of the anatase-semiconductor cores.[7,9]

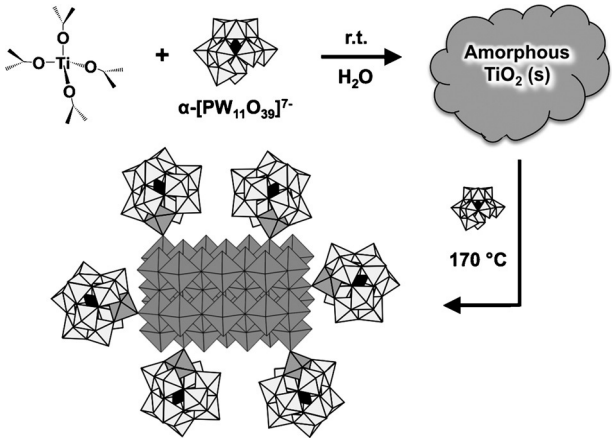

Scheme 1. Direct coordination of Ti^{IV}-substituted POM cluster anions to anatase-TiO_2 cores. The reaction of amorphous TiO_2(s) (upper right) with the mono-defect Keggin anion, $\alpha\text{-}PW_{11}O_{39}^{7-}$ (**1**; white: W^{VI}-centered polyhedra; black: P^V-centered tetrahedra), gives a clear solution of 6 nm anatase-TiO_2 cores solubilized by covalently attached POM capping ligands, $[\alpha\text{-}PW_{11}O_{39}Ti]\text{-}O^-$ (Ti^{IV}-centered polyhedra are in gray).

[*] Dr. M. Raula, G. Gan Or, M. Saganovich, Dr. O. Zeiri, Prof. I. A. Weinstock
Department of Chemistry, Ben Gurion University of the Negev and the Ilse Katz Institute for Nanoscale Science & Technology
Beer Sheva, 84105 (Israel)
E-mail: iraw@bgu.ac.il
Homepage: http://www.bgu.ac.il/~iraw
Prof. Y. Wang
School of Chemistry and Chemical Engineering
Shandong University, Ji'nan 250100 (China)
Dr. M. R. Chierotti, Prof. R. Gobetto
Department of Chemistry and NIS Centre
University of Turin, Via P. Giuria n° 7, Torino, 10125 (Italy)

[**] I.A.W. thanks the Israel Science Foundation (ISF; 190/13), the ISF & Planning and Budgeting Committee (I-CORE Program 152/11), and the Adelis Foundation, and M.R. thanks the PBC for a Fellowship.

Supporting information for this article is available on the WWW under http://dx.doi.org/10.1002/anie.201501941.

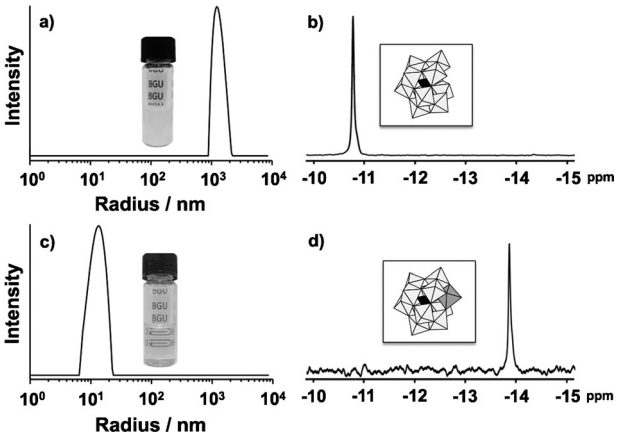

Figure 1. Dynamic light scattering (DLS) data (a, c) and ^{31}P NMR spectra (b, d) before (a, b) and after (c, d) reaction of amorphous TiO_2(s) with $Na_7[\alpha\text{-}PW_{11}O_{39}]$ (Na_7**1**). Room-temperature hydrolysis of TTIP (8 mM), in the presence of **1** (4 mM), gives micrometer-sized particles of TiO_2(s) (a and inset) and no change in the ^{31}P NMR spectrum of **1** (−10.8 ppm; b). Heating for 20 h at 170 °C gives a clear solution of nano-scale particles (c and inset) and $[\alpha\text{-}PTiW_{11}O_{40}]^{5-}$ (**2**) is the only POM observed by ^{31}P NMR spectroscopy (−13.9 ppm; d). The full ^{31}P NMR spectrum and a balanced equation are provided in the Supporting Information.

When titanium tetraisopropoxide (TTIP; 8 mM) is added at room temperature to one-half an equivalent of aqueous $Na_7[\alpha\text{-}PW_{11}O_{39}]$ (Na_7**1**; 4 mM, pH 6), rapid hydrolysis of the TTIP gives a cloudy solution containing micrometer-sized particles of amorphous TiO_2(s) (Figure 1a). The pH remains unchanged,[10] as does the ^{31}P NMR spectrum of **1** (Figure 1b). After 20 h at 170 °C, however, a clear pH 6.5 solution of nanosized particles is obtained (Figure 1c), and $\alpha\text{-}PTiW_{11}O_{40}^{5-}$ (**2**),[4e,f,11] a byproduct of the reaction, is the only POM observed by ^{31}P NMR spectroscopy (Figure 1d).

The nanosized TiO_2-based particles differ dramatically from traditional examples of electrostatically stabilized colloidal TiO_2. They are indefinitely stable in water over a wide range of pH values (from 2 to 8), giving optically clear solutions in the complete absence of added organic ligands.[12] Even more remarkable is that, like molecular macroanions, they are uniquely resistant to aggregation: after isolation as solids, they can be stored as water-soluble sodium salts.

Isolation and purification were carried out as follows. First, isopropanol and inorganic byproducts (including **2**) were partially removed from the clear reaction mixture (10 mL) by extensive dialysis against pure water. The dialyzed reaction mixture was then made 2 M in NaCl, giving a cloudy solution from which a hydrated white solid was obtained by centrifugation. When 10 mL of pure water was added, the white solid readily dissolved, once again giving a clear solution. The precipitation/redissolution cycle was carried out four times, reducing the amount of free $\alpha\text{-}PTiW_{11}O_{40}^{5-}$ (**2**) to less than 1 pM (based on a dilution factor of ca. 1×10^{10}). The final white solid readily dissolved in water, with the number-weighted average radius having increased by less than 1 nm (by DLS; Supporting Information, Figure S2), and no change in zeta potential (particle charge), which remained constant at −50 mV.

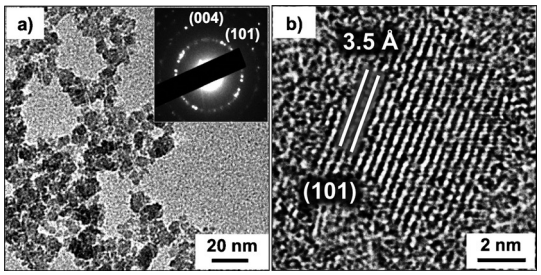

Figure 2. Characterization of anatase-TiO_2 nanocrystal cores. a) TEM image of the purified nanoparticles (dried); inset: selected-area electron diffraction pattern of the particles. b) HRTEM image of a single anatase core with fringes corresponding to (101) planes of Ti atoms.

The TiO_2 cores were characterized by transmission electron microscopy (TEM) and electron and powder X-ray diffraction (XRD). TEM images of dried samples (Figure 2a) revealed an average particle size of 6.9 ± 1.4 nm (based on measurements of 50 particles). Although not morphologically homogeneous, many particles appear to be approximately rectangular prismatic in shape (see the Supporting Information, Figure S3 for more images). Electron diffraction of the particles (inset) featured well-defined rings, indicative of crystalline structure, which when indexed gave a precise match for anatase.[13,14]

Debye–Scherrer[15] analysis of XRD data (Supporting Information, Figure S3) gave an anatase-crystallite size of 6.1 ± 0.2 nm, statistically identical to the average particle size obtained from TEM images. This correspondence between crystallite size (from XRD) and particle size (from TEM) shows that, on average, each metal oxide core is a single nanocrystal of anatase TiO_2.[14] Finally, high-resolution TEM (HRTEM) images of the nanocrystals (NCs) revealed exposed facets with atomic fringes separated by distances matching the d-spacing of the (101) planes of anatase (Figure 2b).[13c]

Next, capping ligands on the surfaces of the anatase NCs were observed by cryogenic TEM (cryo-TEM) and high-angle annular dark field (HAADF) imaging. Cryo-TEM images (Figure 3a)[16] revealed numerous circa 1 nm diameter clus-

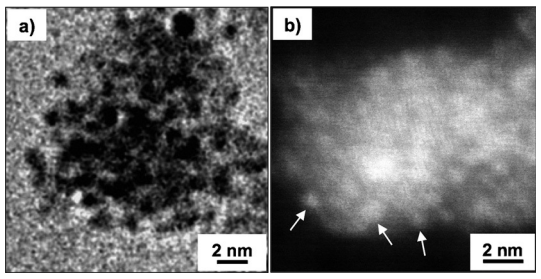

Figure 3. Tungsten-based capping ligands on individual anatase-TiO_2 cores. a) Cryo-TEM image of numerous ca. 1 nm clusters (dark objects) on the surface of an anatase NC (for comparison, images of anatase with no surface-attached clusters are provided in the Supporting Information, Figure S4). b) High-angle annular dark field (HAADF) image of the ca. 1 nm clusters on an anatase NC. EDX data (Supporting Information, Figure S5), showed that the numerous bright-white spots (three of which are indicated by arrows) are tungsten based, while the gray areas are mostly titanium.

ters at the surfaces of the anatase cores (see the Supporting Information, Figure S4 for additional images). To our knowledge, this is the first reported image of capping ligands on a soluble metal oxide nanocrystal. The 1 nm clusters were further analyzed by HAADF imaging of a dried sample (Figure 3b), which again revealed numerous circa 1 nm objects, now appearing as white objects on a darker background. Consistent with heavier elements giving rise to brighter regions in HAADF images, data from energy-dispersive X-ray (EDX) spectroscopy (0.4 nm^2 spot analysis) showed the 1 nm objects to be tungsten-based (Supporting Information, Figure S5).

The large abundance of tungsten-based clusters made it possible to obtain a definitive vibrational spectrum of these capping ligands (Figure 4). After correcting the background for absorbance by anatase (Supporting Information, Figure S6), the solid-state FTIR spectrum of the purified material (——) was strikingly similar to that of α-$PTi^{IV}W_{11}O_{40}^{5-}$ (**2**, -----).

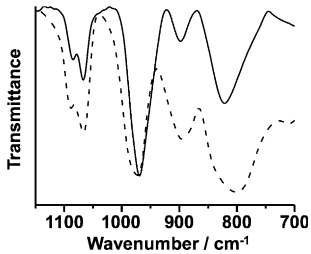

Figure 4. Spectroscopic characterization of the heteropolytungstate capping ligands. FTIR spectra of (——): the heteropolytungstate-capped anatase (corrected for absorbance by TiO_2), and (-----): pure $Na_5[\alpha\text{-}PTiW_{11}O_{40}]$ (Na_5**2**).

Both featured two P–O stretching bands, at 1066 and 1085 cm^{-1}, which are diagnostic for derivatives of the mono-defect ion, α-$PW_{11}O_{39}^{7-}$ (**1**), whose central PO_4 units possess local C_{3v} symmetry. The 20 cm^{-1} separation between these two bands is much smaller however than the circa 40 cm^{-1} separation observed for **1** (1085 and 1041 cm^{-1}), and unambiguously signifies in-pocket occupancy of the defect site by a metal cation, that is, M^{n+} in $[\alpha\text{-}PM^{n+}W_{11}O_{39}]^{(7-n)-}$.[17] In the present case, M^{n+} can only be Ti^{IV}. The terminal W=O stretch (at 970 cm^{-1}) is also characteristic of M^{n+}-substituted ions; in the parent ion, **1**, this band occurs at a much lower energy (950 cm^{-1}). Particularly striking is that in both spectra the band at 1066 cm^{-1} is more intense than is that at 1085 cm^{-1}, a signature that is characteristic of **2**.

The P^V heteroatom was quantified by X-ray photoelectron spectroscopy (XPS), which analyzes the particle surfaces to a depth of several nm. It gave integrated signal intensities for P 2p and W 4d in an atomic ratio of 1 P per 12 ± 2 W, which is statistically identical to the 1:11 ratio in **2**.[18] The presence of P^V was further confirmed by solid-state ^{31}P NMR spectroscopy (for the complete solid-state NMR analysis, see the Supporting Information and Figure S7).

The POM capping ligand was independently identified by electrospray ionization mass spectroscopy (ESI-MS). For this, concentrated HCl was used to dissolve the TiO_2 cores (2 h at 90 °C), giving a clear solution of Ti^{IV} ions[19] and liberated POM-capping ligands.[20] Tetrabutylammonium bromide (TBABr) was then added to selectively precipitate the POM as the corresponding TBA salt. After collection of the solid by centrifugation and dissolution in MeCN, ESI-MS revealed $\{TBA_5H[PTiW_{11}O_{40}]\}^+$, with an envelope centered at 3953.59, which is nearly identical to the simulated value of 3953.61 (Figure 5; see the Supporting Information, Figure S8 for additional MS data).

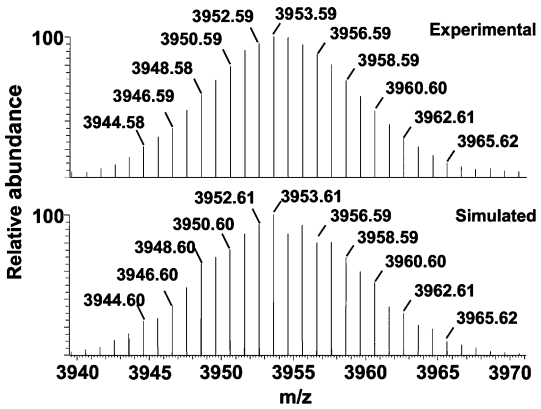

Figure 5. ESI mass spectra for the $z = +1$ ion, $\{TBA_5HP[TiW_{11}O_{40}]\}^+$, a mixed TBA/$H^+$ salt of $[PTiW_{11}O_{40}]^{5-}$ (**2**). The instrument accuracy is ±0.1 amu.

Extensive coverage of the anatase surfaces by Ti^{IV}-substituted Keggin ions closely related to **2** was supported by wide-area EDX analysis of the bulk material, which gave an atom-percent composition of 25 ± 3 % W to 75 ± 3 % Ti (Supporting Information, Figure S9). Notably, these values correspond to the percentages obtained by simple calculation. If each cluster anion is allocated a reasonable[21] 1.8 nm^2 footprint on the anatase surface, an average of 55 ± 10 undecatungstate-based clusters (600 ± 110 W atoms) are present on each ca. 6 nm (1800 ± 550 Ti-atom) anatase core (Supporting Information, Table S1). The zeta potential of the NCs, −50 mV, assigns a net charge of 15 e for each assembly,[22] such that, like POM monolayers on gold nanoparticles,[23] most of the (hydrated) Na^+ countercations must lie between the closely separated cluster anions.

Although closely related to $[\alpha\text{-}PTi^{IV}W_{11}O_{40}]^{5-}$ (**2**), the POM capping ligands (heretofore designated **2′**) are directly coordinated to the anatase NCs. This was supported by seven lines of evidence: 1) No aggregation of the NCs was observed by DLS after 14 days of dialysis against pure water (Supporting Information, Figure S2). The pH was nearly identical to the isoelectric point of anatase (pH 6.7), at which its colloids typically precipitate from water.[24] If the **2′** cluster anions were electrostatically associated with the TiO_2 NCs, the POM anions would be inherently labile, such that extensive dialysis would eventually remove them from the NC surface, leaving unprotected particles that would certainly precipitate at near-neutral pH. In the present case, however, the solution remained optically clear. Thus, unlike traditional colloids

with electrostatically associated stabilizing ions, the **2′** cluster anions are not labile. 2) After repeated cycles of precipitation (in 2 M NaCl), centrifugation and redissolution, the isolated NCs readily dissolve in pure water to give clear solutions. This is in stark contrast to the insoluble solids obtained when traditional colloids are similarly treated. 3) Upon drying, the POM ligands remain tightly bound to the TiO_2 NCs, giving HAADF images of intact structures (Figure 3b), closely resembling those imaged in their vitrified solution-like state by cryo-TEM (Figure 3a). 4) The repeated NaCl treatments had no effect on the net charges of the nanoparticles: zeta-potential values remained unchanged (−50 mV). 5) The solubility of the NCs in water increased twenty-fold (from 5 to 100 mM Ti) when the Na^+ counter cations were replaced by Li^+, while 6) replacement of Na^+ by organic counter cations, (n-Bu_4N^+ and n-Octyl$_4N^+$), gave organic-solvent-soluble analogues: After adding $(n\text{Bu})_4\text{NBr}$ to precipitate the **2′**-capped NCs from water, the resultant white solid readily dissolved in MeOH, giving a clear solution (see the Supporting Information, Figure S10 for DLS and TEM data). Analogous n-Octyl$_4N^+$ salts dissolved in toluene, CH_2Cl_2, MeCN, and THF. 7) In a final definitive experiment, no anion-exchange was observed when **2′**-capped anatase NCs were reacted with [α-$AlW_{12}O_{40}]^{5-}$ (1 mM; ca. 600 times the concentration of the NCs, and 10 times that of surface-bound **2′** ligands; Supporting Information, Figure S11).[25] None of these findings is compatible with electrostatic association of POMs to the anatase NCs; they can only be understood as the result of a unique situation in which **2′** capping ligands are directly coordinated (covalently attached) to the anatase surface.

This conclusion goes hand-in-hand with the partial consumption of amorphous TiO_2(s) by **1** during synthesis (Scheme 1), and with the tendency for Ti^{IV} ions to form stable oxo-bridged structures. Namely, at 170 °C, **1** initially consumes TiO_2(s) by serving as a pentadentate ligand for the titanyl ion, $Ti{=}O^{2+}$, giving freely solvated **2** (Figure 1d). At completion of the reaction, however, numerous POM-ligated Ti^{IV} atoms must remain coordinated to the anatase surface. Consistent with this, the Ti=O ligand in **2** readily forms μ-O linkages to other Ti^{IV} ions as, for example,[11] in [(α-$PW_{11}O_{39}Ti)_2$-μ_2-O]$^{8-}$. Based on this, and by analogy to alkoxide (RO^-) ligands on molecular TiO_2 clusters,[6] 1 nm [α-$PW_{11}O_{39}Ti$]–O^- capping groups might be coordinated to the anatase suface via [α-$PW_{11}O_{39}Ti$]-μ_2-O^- linkages to single Ti atoms (upper right in Figure 6a), or via [α-$PW_{11}O_{39}Ti$]-μ_3-O^- linkages to two Ti atoms (left in Figure 6a). Further studies will address this issue, which might only be resolved by single-crystal X-ray diffraction of molecular analogues with smaller TiO_2 cores.[26]

Meanwhile, unlike simple alkoxide capping ligands, **2′** is redox active, serving as a well-behaved electron acceptor.[27] This was demonstrated using a 1.7 μM solution of **2′**-capped anatase NCs in 200 mM $LiClO_4$ (Figure 6b; Supporting Information, Figure S13). Differential pulse voltammetry (DPV; a technique much more sensitive than cylic voltammetry) gave definitive cathodic currents with maxima at ca. −565 and −790 mV, followed by corresponding anodic currents, indicating that the capping ligands are cleanly reduced and re-oxidized on the anatase surface.[28]

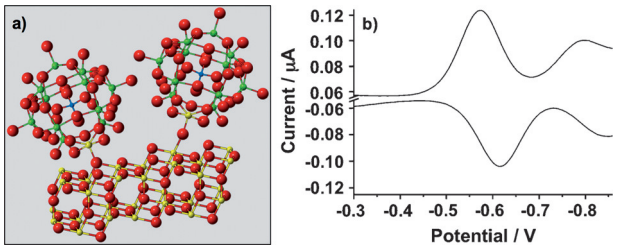

Figure 6. Coordination modes and redox chemistry of POM capping ligands on anatase nanocrystals. a) By analogy to alkoxide ligands on molecular TiO_2 clusters, **2′** is shown bound via μ_2-O or μ_3-O linkages to a facet perpendicular to (101) planes of anatase (O: red, Ti: yellow, W: green). b) Forward and reverse differential pulse voltammograms (versus Ag/AgCl, 3 M NaCl) of **2′**-capping ligands on anatase nanocrystals in 0.2 M aqueous $LiClO_4$.

Moreover, the redox properties of the POM capping ligands can be rationally tuned. This was demonstrated by reacting amorphous TiO_2(s) with α-$SiW_{11}O_{39}^{8-}$ (K^+ salt), thus increasing the negative charges of the resulting capping ligands by one unit (characterization data are given in the Supporting Information, Figure S14). Consistent with established correlations between anion charge and reduction potential,[29] the first cathodic wave was shifted by ca. 175 mV in the negative direction (Supporting Information, Figure S14f).[30]

Finally, the reduction potential of the POM ligand has a profound effect on photocatalytic activity. For example, under UV irradiation (150 W Xe lamp) in 10 vol% MeOH in water, H_2 evolution proceeds at 725 μmol g^{-1} h^{-1} for [α-$SiW_{11}O_{39}Ti$]-O^--capped NCs (per g of TiO_2), and increases to 1500 μmol g^{-1} h^{-1} for the **2′**-capped NCs (Figure 7; see the Supporting Information for details). These rates are an order of magnitude larger than the values of 78 and 138 μmol g^{-1} h^{-1} obtained under identical conditions for commercial anatase and pure **2**, respectively, revealing dramatically enhanced reactivity upon covalent attachment of the POMs to the TiO_2-NC cores.

Interestingly, the **2′**-capped NCs are much more effective than the [α-$SiW_{11}O_{39}Ti$]-O^--capped NCs. The **2′** ligands possess more positive reduction potentials than the [α-

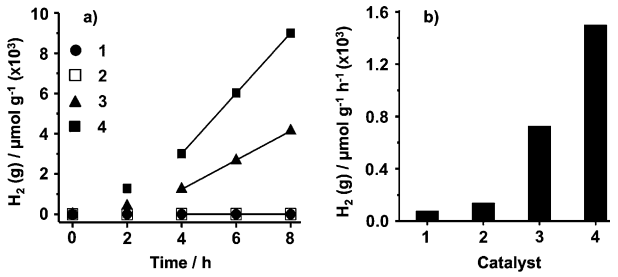

Figure 7. a) Photocatalytic H_2 evolution in as a function of time per gram quantity of: 1) commercial anatase, 2) pure [α-$PTiW_{11}O_{40}]^{5-}$ (Na^+ salt), 3) TiO_2 in [α-$SiW_{11}O_{39}Ti$]-O^--capped anatase NCs, and 4) TiO_2 in **2′**-capped anatase NCs. b) Rates of H_2 production, that is, slopes of the lines indicated in panel (a) (all with R^2 values of 0.999), after an induction period observed for both types of POM-capped NCs.

$SiW_{11}O_{39}Ti]–O^-$ ligands, and hence, are more effective electron acceptors. In principle, this could facilitate charge separation under photocatalytic conditions by more efficiently "trapping" photoexcited electrons. While future studies will address this in detail, the POM ligands could play an electron-accepting role analogous to that of platinum(0) nanoparticles routinely deposited on TiO_2 for numerous applications.[31] Unlike platinum(0), however, the electron-accepting properties of the POM ligands can be rationally tuned.

In summary, direct coordination of numerous polyoxometalate cluster anions to the surfaces of anatase-TiO_2 nanocrystals gives stable macroanion-like assemblies, which can be isolated as their alkali-metal cation or n-R_4N^+ salts, and subsequently re-dissolved in water or organic solvents. And, just as traditional ligands control catalytically active metal centers in molecular complexes, the tunable redox chemistry of covalently attached POM capping ligands provides new options for rationally modifying the reactions of metal oxide semiconductor cores. More generally, the covalent attachment of redox-active POM capping ligands to nanocrystals of titanium and other transition-metal oxides promises access to a new family of catalytically active assemblies uniquely situated at the interface between molecular macroanions and traditional colloidal nanoparticles.

Keywords: electron transfer · hybrid materials · nanostructures · polyoxometalates · titanium dioxide

How to cite: *Angew. Chem. Int. Ed.* **2015**, *54*, 12416–12421
Angew. Chem. **2015**, *127*, 12593–12598

[1] For references to a wide variety of structures and applications, see: *special issue on Polyoxometalate Cluster Science,* (Eds.: L. Cronin, A. Müller), *Chem. Soc. Rev.* **2012**, *41*, 7325–7648.
[2] a) K. Nomiya, Y. Sakai, S. Matsunaga, *Eur. J. Inorg. Chem.* **2011**, 179–196; b) T. McGlone, L. Vila-Nadal, H. N. Miras, D.-L. Long, J. M. Poblet, L. Cronin, *Dalton Trans.* **2010**, *39*, 11599–11604; c) E. M. Villa, C. A. Ohlin, W. H. Casey, *J. Am. Chem. Soc.* **2010**, *132*, 5264–5272; d) G. A. Al-Kadamany, F. Hussain, S. S. Mal, M. H. Dickman, N. Leclerc-Laronze, J. Marrot, E. Cadot, U. Kortz, *Inorg. Chem.* **2008**, *47*, 8574–8576; e) R. J. Errington, S. S. Petkar, P. S. Middleton, W. McFarlane, W. Clegg, R. A. Coxall, R. W. Harrington, *Dalton Trans.* **2007**, 5211–5222; f) L. G. Detsuheva, M. A. Fedotov, L. I. Kuznetsova, A. A. Vlasov, V. A. Likholobov, *Russ. Chem. Bull.* **1997**, *46*, 874–880; g) T. Yamase, T. Ozeki, H. Sakamoto, S. Nishiya, A. Yamamoto, *Bull. Chem. Soc. Jpn.* **1993**, *66*, 103–108; h) P. J. Domaille, W. H. Knoth, *Inorg. Chem.* **1983**, *22*, 818–822; i) C. Tourne, *C. R. Acad. Sci., Paris, Ser. C* **1968**, *266*, 702–704.
[3] T. Yamase, M. Sugeta, *Inorg. Chim. Acta* **1990**, *172*, 131–134.
[4] a) O. A. Kholdeeva, *Eur. J. Inorg. Chem.* **2013**, *2013*, 1595–1605; b) N. S. Antonova, J. J. Carbo, U. Kortz, O. A. Kholdeeva, J. M. Poblet, *J. Am. Chem. Soc.* **2010**, *132*, 7488–7497; c) Y. Goto, K. Kamata, K. Yamaguchi, K. Uehara, S. Hikichi, N. Mizuno, *Inorg. Chem.* **2006**, *45*, 2347–2356; d) C. N. Kato, S. Negishi, K. Yoshida, K. Hayashi, K. Nomiya, *Appl. Catal. A* **2005**, *292*, 97–104; e) O. A. Kholdeeva, G. M. Maksimov, R. I. Maksimovskaya, L. A. Kovaleva, M. A. Fedotov, V. A. Grigoriev, C. L. Hill, *Inorg. Chem.* **2000**, *39*, 3828–3837; f) T. Yamase, E. Ishikawa, Y. Asai, S. Kanai, *J. Mol. Catal. A* **1996**, *114*, 237–245.
[5] Y. Sakai, K. Yoza, C. N. Kato, K. Nomiya, *Chem. Eur. J.* **2003**, *9*, 4077–4083.
[6] a) P. Coppens, Y. Chen, E. Trzop, *Chem. Rev.* **2014**, *114*, 9645–9661; b) L. Rozes, C. Sanchez, *Chem. Soc. Rev.* **2011**, *40*, 1006–1030.
[7] R. C. Snoeberger, K. J. Young, J. Tang, L. J. Allen, R. H. Crabtree, G. W. Brudvig, P. Coppens, V. S. Batista, J. B. Benedict, *J. Am. Chem. Soc.* **2012**, *134*, 8911–8917.
[8] These too are undergoing rapid development. For impressive examples, see: J. Huang, W. Liu, D. S. Dolzhnikov, L. Protesescu, M. V. Kovalenko, B. Koo, S. Chattopadhyay, E. V. Shenchenko, D. V. Talapin, *ACS Nano* **2014**, *8*, 9388–9402.
[9] For recent advances in electron-transfer reactions of TiO_2 and Fe_3O_4 nanoparticles, respectively, see: a) J. N. Schrauben, R. Hayoun, C. N. Valdez, M. Braten, L. Fridley, J. M. Mayer, *Science* **2012**, *336*, 1298–1301; b) J. J. P. Roberts, J. A. Westgard, L. M. Cooper, R. W. Murray, *J. Am. Chem. Soc.* **2014**, *136*, 10783–10789.
[10] As shown in Scheme 1, the four H^+ ions liberated by the hydrolysis of TTIP are consumed by the isopropoxide ligands, giving four equivalents of isopropanol with no change in the pH of the solution.
[11] a) Y. Matsuki, Y. Mouri, Y. Sakai, S. Matsunaga, K. Nomiya, *Eur. J. Inorg. Chem.* **2013**, 1754–1761; b) G. Maksimov, R. Maksimovskaya, O. Kholdeeva, M. Fedotov, V. Zaikovskii, V. Vasil'ev, S. Arzumanov, *J. Struct. Chem.* **2009**, *50*, 618–627.
[12] U. Vukičević, S. Ziemian, A. Bismarck, M. S. P. Shaffer, *J. Mater. Chem.* **2008**, *18*, 3448–3453.
[13] a) Y. Rao, B. Antalek, J. Minter, T. Mourey, T. Blanton, G. Slater, L. Slater, J. Fornalik, *Langmuir* **2009**, *25*, 12713–12720; b) Joint Committee on Powder Diffraction Standards, Powder Diffraction File, Card No. 21–1272; c) Y. Liao, W. Que, Q. Jia, Y. He, J. Zhang, P. Zhong, *J. Mater. Chem.* **2012**, *22*, 7937–7944.
[14] D. B. Williams, C. B. Carter, *Transmission Electron Microscopy: A Textbook for Materials Science*, 2nd ed., Springer, New York, **2009**.
[15] H. P. Klug, L. E. Alexander, *X-Ray diffraction Procedures*, 2nd ed., Wiley, New York, **1974**.
[16] Although not clearly discerned in TEM or HRTEM images of dry samples, cryo-TEM imaging effectively reveals the more-electron-dense 1 nm polytungstate ligands.
[17] C. Rocchiccioli-Deltcheff, R. Thouvenot, *J. Chem. Res. Syn.* **1977**, 46–47.
[18] Relative to the bulk mateial (that is, which would include the mass of TiO_2), the reported uncertainty is equivalent to ±0.1 mass% P.
[19] G. Schwarzenbach, J. Muehlebach, K. Mueller, *Inorg. Chem.* **1970**, *9*, 2381–2390.
[20] The ^{31}P NMR spectrum (after overnight acquisition) contains a sharp signal at −13.96 ppm, precisely as expected for $[PTiW_{11}O_{40}]^{5-}$ (**2**) upon acid condensation in strongly acidic solution (Supporting Information, Figure S8).
[21] a) O. Zeiri, Y. Wang, A. Neyman, F. Stellacci, I. A. Weinstock, *Angew. Chem. Int. Ed.* **2013**, *52*, 968–972; *Angew. Chem.* **2013**, *125*, 1002–1006; b) Y. Wang, O. Zeiri, A. Neyman, F. Stellacci, I. A. Weinstock, *ACS Nano* **2012**, *6*, 629–640; c) Y. Wang, A. Neyman, E. Arkhangelsky, V. Gitis, L. Meshi, I. A. Weinstock, *J. Am. Chem. Soc.* **2009**, *131*, 17412–17422.
[22] The calculation was carried out as shown in Ref. [21c].
[23] a) Y. Wang, I. A. Weinstock, *Chem. Soc. Rev.* **2012**, *41*, 7479–7496; b) Y. Wang, O. Zeiri, S. Sharet, I. A. Weinstock, *Inorg. Chem.* **2012**, *51*, 7436–7438.
[24] X.-Q. Chen, W.-H. Shen, *Chem. Eng. Technol.* **2008**, *31*, 1277–1281.
[25] After 3 h at room temperature, the NCs were removed by precipitation (by NaCl addition and centrifugation), and the supernatant solution was concentrated from 10 to 3 mL and treated with H_2O_2. If the **2′** cluster anions were electrostatically associated with the NCs, anion exchange with the relatively large

concentration of $[\alpha\text{-}AlW_{12}O_{40}]^{5-}$ would have caused extensive release of **2′** to the bulk solution. However, no titanium–peroxo complexes **3** were detected by UV/Vis spectroscopy (Supporting Information, Figure S11). Notably, exchange of only about 5% of the POM ligands **2′** would have given rise to a detectable absorbance band at 400 nm.

[26] The situation is similar to that of alkanethiolate-protected Au nanoparticles (RS-Au NPs): Many years, and thousands of published articles, after discovery of the RS-Au NPs themselves, the "staple" motif of RS binding was determined from molecular $Au_{25}(SR)_{18}$ and $Au_{102}(SR)_{44}$ clusters; see, respectively: a) M. W. Heaven, A. Dass, P. S. White, K. M. Holt, R. W. Murray, *J. Am. Chem. Soc.* **2008**, *130*, 3754 – 3755; b) P. D. Jadzinsky, G. Calero, C. J. Ackerson, D. A. Bushnell, R. D. Kornberg, *Science* **2007**, *318*, 430 – 433.

[27] Functionalized organic ligands are now being investigated as electron-donating sensitizers for molecular TiO_2 clusters; see Ref. [7].

[28] The implied current amplification may be an ensemble effect, as in: C. A. Beasley, R. W. Murray, *Langmuir* **2009**, *25*, 10370 – 10375.

[29] a) O. Snir, Y. Wang, M. E. Tuckerman, Y. V. Geletii, I. A. Weinstock, *J. Am. Chem. Soc.* **2010**, *132*, 11678 – 11691; b) J. J. Altenau, M. T. Pope, R. A. Prados, H. So, *Inorg. Chem.* **1975**, *14*, 417 – 421.

[30] For comparison, the first one-electron reduction potential of $\alpha\text{-}SiW_{12}O_{40}^{4-}$ is about 190 mV more negative than that of $\alpha\text{-}PW_{12}O_{40}^{3-}$.

[31] J. Schneider, M. Matsuoka, M. Takeuchi, J. Zhang, Y. Horiuchi, M. Anpo, D. W. Bahnemann, *Chem. Rev.* **2014**, *114*, 9919 – 9986.

Received: March 1, 2015
Published online: April 20, 2015

